Supplemental Material

Figures

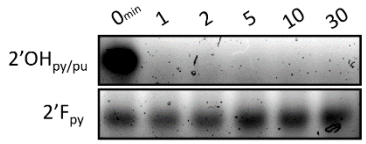

Supplemental 1. RNase stability of 2'hydroxylated and 2'fluorinated pyrimidine Broccoli RNAs. Each construct was incubated with purified RNase A for given time before being quenched with EDTA and loading dye. Broccoli transcribed with 100% 2'OH rNTPs (2'$OH_{py/pu}$) was completely degraded within 1min of RNase A exposure, whereas the incorporation of 2'F pyrimidine NTPs resulted in no visible degradation for more than 30minutes.

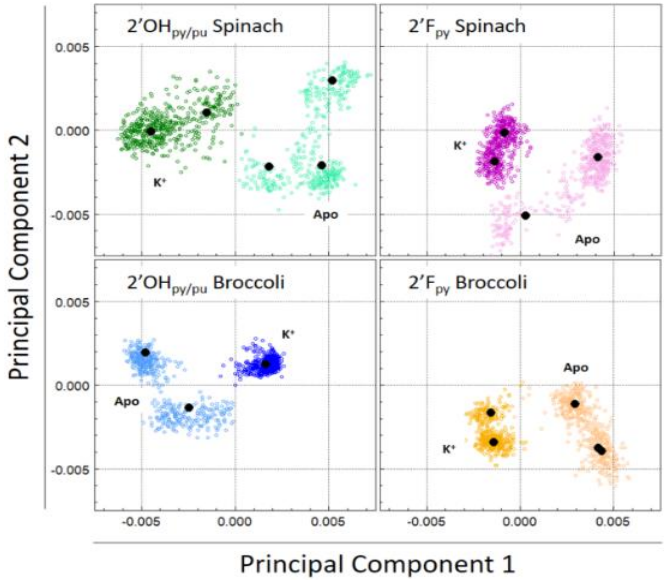

Supplemental 2. 250ns Molecular dynamic simulations were performed to observe structural differences between 2'chemistries in Spinach and Broccoli over time. Principal component analysis of G-quadruplex motifs under 3 variable conditions are presented (RNA identity, 2'chemistry, and K^+ coordination). Each colored dot corresponds to one G-quadruplex structure, sampled every 100ps; Black dots correspond to the structural average of each unique population.

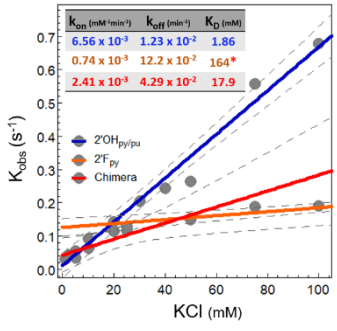

Supplemental 3. Chimera K^+ binding kinetics. Following the identical protocol described for 2'$OH_{py/pu}$ and 2'F_{py}, 0.25μM Chimera was incubated with various KCl concentrations, and tripartite complex formation was observed by fluorescence. Fluorescent traces of individual KCl concentrations were fit to acquire K_{obs} values. These K_{obs} are plotted above against their respective KCl concentrations, overlaid with identical data for 2'$OH_{py/pu}$ and 2'F_{py} monomers adapted from figure 2. The Chimera behaves as a mixture of the two component monomers, as expected.

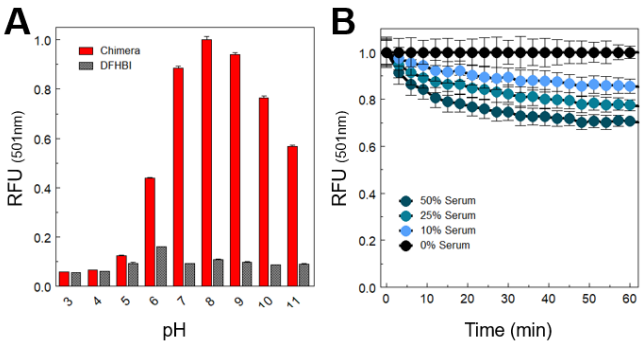

Supplemental 4. Assessment of Chimera stability. (A) pH-dependent fluorescence of Chimera shows construct displays maximal complex fluorescence at pH 8. (B) Chimera fluorescence was observed over time in the presences of increasing cell culture serum concentrations, 10, 25, and 50% by volume. Buffer and KCl concentrations held constant for each serum concentration. Serum was a 1:1 mixture of Bovine Growth Serum and Fetal Calf Serum.

Table 1. Comparative traits of published fluorescent K^+ sensors. Values as reported in stated supplemental references.

Name	Chemistry	K_D (mM)	Functional Range (mM)	λ Fluorescent Emission (nm)	Reference
NK1	Small Molecule	200	10-50	572	1
KS6	Small Molecule	—	30-500	540	2
TAC	Small Molecule	—	—	540	3
TAC-Red	Small Molecule	—	0-50	574	4
TAC-Chrimson	Small Molecule	—	20-60	600	5
PBFI	Small Molecule	8	—	500	6
CDC222	Small Molecule	15-34	2.5-6.5	445	7
GEPII (family)	Protein	0.1-20	0.01-1000	550	8
KIRIN1	Protein	1.67	0.1-10	530	9
GINKO	Protein	0.4	3-100	514	9
PSO-1	DNA	—	—	581	10
PSO-2	DNA	7.3	0.5-10	480	11
TBA	DNA	—	100-200	583	11
Broccoli Chimera	RNA (Modified)	8-18	0.15-100	501	—

Methods

In vitro Transcription and purification: RNA transcripts were prepared using linear dsDNA PCR templates. Sequences of the forward DNA strand are as follows (T7 promoter is underlined, construct in bold font): Spinach 5'—GCGCGCGAATTCTAATACGACTCACTATA**GGAGGACGCGACCGAAATGGTGAAGGACGGGTCCAGTGCGAAACACGCACTGTTGAGTAG**AGTGTGAGCTCCGTAACTGGTCGCGTC—3'; and Broccoli 5'—GCGCGCGAATTCTAATACGACTCACTATA**GGGAGACGGTCGGGTCCAGGCACACAAAAATGTTGCCTGTTGAGTAGAGTGTGGGCTCC**—3'. Prior to transcription, PCR templates were gel purified, phenol:chloroform cleaned, and desalted, similar to RNA clean

up (described below). Transcription reactions were assembled at room temperature in the following order, to final concentrations of: water, 1X T7 RNAP transcription buffer (NEB), 24mM $MgCl_2$, 4mM each NTP (2'OH purines from NEB, 2'F pyrimidines from Trilink Biotechnologies), 15-25ng/µl dsDNA, 5mM DTT, 1U/µl murine RNase inhibitor (NEB), 2.5mU/µl Yeast Inorganic Pyrophosphatase (NEB), 5U/µl WT T7 RNA polymerase (NEB) or 1.25U/µl mutant T7 R&D polymerase (Lucigen, Inc). RNA was transcribed at 42°C for 2-5 hours. Transcriptions were quenched with DNase I treatment, and observed on a 4% agarose sodium borate gel, stained with Sybr Gold nucleic acid dye. Target transcript bands were purified by gel excision and electro-eluted into 3.5kDa MWCO dialysis tubing. RNA was concentrated with a 3.5KDa MWCO concentrating spin column (Millipore) or Speed Vac, and cleaned with acidified phenol:chloroform:isoamyl alcohol (Ambion). RNA was then desalted into 5mM Tris (pH 8.0) using a 7kDa MWCO desalting spin column (Zeba, Thermo Scientific), and quantified by UV-absorbance at 260nm and fluorescence (Qubit HS RNA kit; Invitrogen), and stored at -80°C. Prior to experimental use of frozen stocks, RNA was folded following a basic protocol: dilution into reaction buffer, then successive thermocycler incubations at 95°C (20sec), 50°C (10sec), 37°C (10sec), addition of DFHBI, 4°C (≥30min).

Fluorescence: Single sample fluorescent measurements were performed on a Photon Technologies International QM-1 steady state fluorescent spectrophotometer. All fluorescent measurements were performed with the following solution with various cation additions: 0.5µM RNA, 20mM Tris (pH 8.0), 5mM $MgCl_2$, 20µM DFHBI. Samples were read at 20°C, held constant by a circulating water bath, and excited at 468nm in a 2mm quartz fluorescence cuvette. KCl titrations were performed by folding RNA in the presence of various KCl concentrations in individual reaction tubes. Samples were then incubated on ice for 2hr to ensure equilibrium was reached.

RNaseA-dependent stability: 0.5µM RNA was incubated with 1.25mU/µl purified RNase A (Qiagen). At stated time points, 5µl of reaction was removed, quenched with 10mM EDTA in 2X gel loading dye, and frozen at -20°C. Samples were analyzed via 4% agarose gel stained with Sybr Gold nucleic acid dye.

pH-dependent stability: 0.5µM Chimera was assayed for fluorescent yield at 9 pH points in a universal buffer composed of 20mM acetate, 20mM HEPES, 20mM Borate, 100mM KCl, 5mM $MgCl_2$, 20mM DFHBI. Samples were incubated at stated pH for 30minutes, then analyzed simultaneously in a SpectroMax M2^e Microplate reader (Molecular Devices), Ex/Em at 468/501nm, respectively.

Serum-dependent Stability: 0.5µM Chimera was assayed for fluorescence over time in increasing concentrations of cell culture serum, 0, 10, 25, and 50%. Serum was composed of a 1:1 mixture of Bovine Growth Serum and Fatal Calf Serum (Atlanta Biologicals). Fluorescence was measured in a SpectroMax M2^e Microplate reader (Molecular Devices). Samples were Top-read at 25°C, every 60 seconds for 60min with Ex/Em at 468/501nm. Data plotted in GraphPad Prism 5.

Tripartite complex association kinetics: Kinetic fluorescence was performed by rapid, in-cuvette mixing of folded Apo-state 0.25µM RNA in buffer with a 10% volume of 10X KCl in water. Emission was read at 501nm every 29.75 seconds with a 0.25 second shutter exposure. Association curves of individual KCl concentrations were fit in GraphPad Prism 5 using the following built in equation for specific binding:

$$Y = [(B_{max})(X)]/(K_D+X) \quad (1)$$

This fit assumes any non-specific binding does not contribute to fluorescence. Individual kinetic fits provided K observed (K_{obs}) rate values. To determine the individual kinetic parameters of the K_{obs} (binding and unbinding, or K_{on} and K_{off}, respectively), K_{obs} values for each KCl concentration were plotted against their respective KCl concentration. Linear regression of the resulting plot provides K_{on} and K_{off}, via the slope and y-intercept, respectively.

Circular Dichroism: Measurements were collected with an Aviv 215 CD Spectrophotometer at 20°C. RNA samples were assayed in 10mM Cacodylate (pH 7.4), 100mM KCl, 5mM $MgCl_2$. RNA was folded as described. 135ng/µl RNA samples were scanned in 1mm quartz CD cuvette from 320 to 190nm by a 0.2nm step, with a 3 second integrated read per step. Data presented as average of three individual scans. Control scans of buffer were subtracted from spectra. Values plotted in GraphPad Prism 5.

Construct Design: Complementary 3' extensions were engineered into Broccoli construct by PCR. The two sequences added to the 3' terminus of dsDNA T7 Broccoli constructs: (1) 5'-**AGACAGACAGT**-3' and (2) 5'-**ACTGTCTGTCT**-3'.

Cell Culture: HEK293T cells were cultured in DMEM with 10% fetal bovine serum, penicillin and streptomycin, and supplemented 5mM glutamine, at 37°C with 5% CO2. Cells were maintained between 40-80% confluent between passages.

Hypotonic Lysis: HEK293T cells were cultured to various degrees of confluence in 96-well, clear-bottom, black-walled, tissue culture plates. Cells were quickly and gently washed once with 1X PBS then once with hypotonic buffer (20mM Tris pH 8.0, 5mM $MgCl_2$, 0.01% Triton X-100), before 200ul of hypotonic lysis solution containing 3µM DFHBI, 0.5µM Broccoli chimera RNA, and 80mU/µl murine RNase Inhibitor was added to each well. Plate immediately placed in SpectroMax M2^e Microplate reader (Molecular Devices). Samples were bottom-read at 25°C, every 60 seconds for 60min with Ex/Em at 468/501nm. Positive control wells of varying KCl concentrations with no cells were simultaneously read, as were negative control wells containing either no cells, no RNA, or neither of both. Positive control samples used fit to a simple nonlinear regression model in GraphPad Prism 5:

$$Y = Y_{intercept} + X*Slope \quad (2)$$

Unknown samples values were interpolated from the resulting plot in GraphPad Prism 5.

Molecular Dynamic Simulations: Broccoli structural model adapted from Savage et al, 2020.[12] 2'fluorinated Broccoli structural model was created in the YASARA software package as described.[12,13] Simulations were performed for 50ns at 298K with an improved Berendsen thermostat for temperature control and a "densostat" for pressure control, with an integration time step of 2.5fs. Ionic concentration was 0.9% w/v NaCl concentration; electrostatics were evaluated using Particle Mesh Ewald with an 8Å cut off for long range interactions.[14] A modified AMBER14 force field for RNA was employed.[15]

Model Analysis: *G-Quadruplex bonding analysis:* The distances between hydrogen bond donors and acceptors for each canonical hydrogen bond within the two-plane G-quadruplex motif was analyzed for each snapshot and plotted as a time trace. Distances within 2Å were considered bound via hydrogen

bonding, and interaction distances outside this range were considered unbound.

Principle Component Analysis: The core residues of the G-quadruplex and DHFBI binding pocket were extracted for every simulation snapshot and aligned to the starting broccoli model, to remove any translations and rotations that occurred over the course of the simulation. The MD trajectories for the aptamer with and without K^+ were combined to form a single trajectory upon which a principal component analysis was conducted using ProDy.[16] Cluster analysis was conducted on the projections of all snapshots onto the first three principal components using Wolfram Mathematica FindCluster. The structures corresponding to cluster averages were then back-calculated using the coordinates of individual elements within the cluster in order to find potential intermediate states.

References:

1 J. Ning and Y. Tian, *Sensors Actuators, B Chem.*, 2020, **307**, 127659.
2 X. Kong, F. Su, L. Zhang, J. Yaron, F. Lee, Z. Shi, Y. Tian and D. R. Meldrum, *Angew. Chemie - Int. Ed.*, 2015, **54**, 12053–12057.
3 H. He, M. A. Mortellaro, M. J. P. Leiner, R. J. Fraatz and J. K. Tusa, *J. Am. Chem. Soc.*, 2003, **125**, 1468–1469.
4 P. Padmawar, X. Yao, O. Bloch, G. T. Manley and A. S. Verkman, *Nat. Methods*, 2005, **2**, 825–827.
5 M. Magzoub, P. Padmawar, J. A. Dix and A. S. Verkman, *J. Phys. Chem. B*, 2006, **110**, 21216–21221.
6 A. Minta, R. Y. Tsien, *J Biol Chem.*, 1989, **264**, 19449–19457.
7 H. Szmacinski and J. R. Lakowicz, *Sensors Actuators, B Chem.*, 1999, **60**, 8–18.
8 H. Bischof, M. Rehberg, S. Stryeck, K. Artinger, E. Eroglu, M. Waldeck-Weiermair, B. Gottschalk, R. Rost, A. T. Deak, T. Niedrist, N. Vujic, H. Lindermuth, R. Prassl, B. Pelzmann, K. Groschner, D. Kratky, K. Eller, A. R. Rosenkranz, T. Madl, N. Plesnila, W. F. Graier and R. Malli, *Nat. Commun.*, 2017, **8**, 1–12.
9 Y. Shen, S. Y. Wu, V. Rancic, A. Aggarwal, Y. Qian, S. I. Miyashita, K. Ballanyi, R. E. Campbell and M. Dong, *Commun. Biol.*, 2019, **4**, 18.
10 H. Ueyama, M. Takagi and S. Takenaka, *J. Am. Chem. Soc.*, 2002, **124**, 14286–14287.
11 S. Nagatoishi, T. Nojima, B. Juskowiak and S. Takenaka, *Angew. Chemie*, 2005, **117**, 5195–5198.
12 J. C. Savage, M. A. Davare and U. Shinde, *Chem. Commun.*, 2020, **56**, 2634–2637.
13 J. C. Savage, P. Shinde, H. P. Bächinger, M. A. Davare and U. Shinde, *Chem. Commun.*, 2019, **55**, 5882–5885.
14 T. Darden, L. Perera, L. Li and P. Lee, *Structure*, 1999, **7**, R55–R60.
15 D. Tan, S. Piana, R. M. Dirks and D. E. Shaw, *Proc. Natl. Acad. Sci.*, 2018, **115**, E1346–E1355.
16 A. Bakan, L. M. Meireles and I. Bahar, *Bioinformatics*, 2011, **27**, 1575–1577.